Received: 18 November 2022 | Revised: 6 April 2023 | Accepted: 8 May 2023

DOI: 10.1111/all.15781

Allergy EUROPEAN JOURNAL OF ALLERGY AND CLINICAL IMMUNOLOGY EAACI WILEY

ORIGINAL ARTICLE

Spatial transcriptomics combined with single-cell RNA-sequencing unravels the complex inflammatory cell network in atopic dermatitis

Yasutaka Mitamura[1] | Matthias Reiger[2,3,4] | Juno Kim[1] | Yi Xiao[1,5] | Damir Zhakparov[1,5] | Ge Tan[1] | Beate Rückert[1] | Arturo O. Rinaldi[1] | Katja Baerenfaller[1,5] | Mübeccel Akdis[1] | Marie-Charlotte Brüggen[2,6,7] | Kari C. Nadeau[8,9] | Patrick M. Brunner[10] | Damian Roqueiro[5,11] | Claudia Traidl-Hoffmann[2,3,4,12] | Cezmi A. Akdis[1,2]

[1]Swiss Institute of Allergy and Asthma Research (SIAF), University of Zurich, Davos, Switzerland

[2]CK CARE - Christine Kühne Center for Allergy Research and Education, Davos, Switzerland

[3]Department of Environmental Medicine, Faculty of Medicine, University of Augsburg, Augsburg, Germany

[4]Institute of Environmental Medicine, Helmholtz Zentrum München, Augsburg, Germany

[5]Swiss Institute of Bioinformatics (SIB), Davos, Switzerland

[6]Department of Dermatology, University Hospital Zurich, Zurich, Switzerland

[7]Faculty of Medicine, University Zurich, Zurich, Switzerland

[8]Sean N. Parker Center for Allergy and Asthma Research, Stanford University, Stanford, California, USA

[9]Division of Pulmonary, Allergy and Critical Care Medicine, Department of Medicine, Stanford University, Stanford, California, USA

[10]Department of Dermatology, Icahn School of Medicine at Mount Sinai, New York, New York, USA

[11]Department of Biosystems Science and Engineering, ETH Zurich, Basel, Switzerland

[12]ZIEL, Technical University of Munich, Freising, Germany

Correspondence
Yasutaka Mitamura, Swiss Institute of Allergy and Asthma Research (SIAF), University Zurich, Herman-Burchard-Strasse 9, CH-7265 Davos Wolfgang, Switzerland.
Email: yasutaka.mitamura@siaf.uzh.ch

Funding information
Novartis Research Foundation

Abstract

Background: Atopic dermatitis (AD) is the most common chronic inflammatory skin disease with complex pathogenesis for which the cellular and molecular crosstalk in AD skin has not been fully understood.

Methods: Skin tissues examined for spatial gene expression were derived from the upper arm of 6 healthy control (HC) donors and 7 AD patients (lesion and nonlesion). We performed spatial transcriptomics sequencing to characterize the cellular infiltrate in lesional skin. For single-cell analysis, we analyzed the single-cell data from suction blister material from AD lesions and HC skin at the antecubital fossa skin (4 ADs and 5 HCs) and full-thickness skin biopsies (4 ADs and 2 HCs). The multiple proximity extension assays were performed in the serum samples from 36 AD patients and 28 HCs.

Abbreviations: AD, atopic dermatitis; CCL, C-C motif chemokine ligand; CCR, C-C motif chemokine receptor; COL, collagen; ITGB, integrin beta; LAMP3, lysosome-associated membrane glycoprotein 3; MRC, mannose receptor C; PTPRC, protein tyrosine phosphatase receptor; TNC, tenascin C.

Results: The single-cell analysis identified unique clusters of fibroblasts, dendritic cells, and macrophages in the lesional AD skin. Spatial transcriptomics analysis showed the upregulation of COL6A5, COL4A1, TNC, and CCL19 in COL18A1-expressing fibroblasts in the leukocyte-infiltrated areas in AD skin. CCR7-expressing dendritic cells (DCs) showed a similar distribution in the lesions. Additionally, M2 macrophages expressed CCL13 and CCL18 in this area. Ligand–receptor interaction analysis of the spatial transcriptome identified neighboring infiltration and interaction between activated COL18A1-expressing fibroblasts, CCL13- and CCL18-expressing M2 macrophages, CCR7- and LAMP3-expressing DCs, and T cells. As observed in skin lesions, serum levels of TNC and CCL18 were significantly elevated in AD, and correlated with clinical disease severity.

Conclusion: In this study, we show the unknown cellular crosstalk in leukocyte-infiltrated area in lesional skin. Our findings provide a comprehensive in-depth knowledge of the nature of AD skin lesions to guide the development of better treatments.

KEYWORDS
atopic dermatitis, single-cell transcriptomics, spatial transcriptomics, targeted proteomics

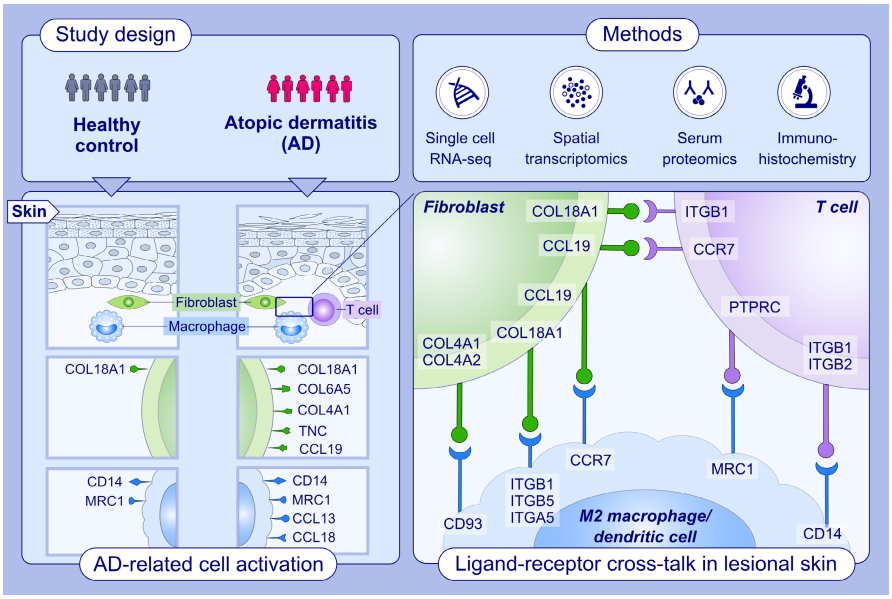

GRAPHICAL ABSTRACT
Single-cell RNA- and spatial RNA-seq identified complex cellular interactionsin lesional skin of AD. COL18A1$^+$ fibroblasts express COL6A5, COL4A1, TNC, and CCL19 and interact with CCR7 positive LAMP3$^+$ dendritic cells and T cells. CCL13$^+$ and CCL18$^+$ M2 macrophages show an interaction with T cells by MRC1-PTPRC and CD14-ITGB1/2. The serum level of TNC and CCL18 shows a positive correlation with AD severity.

1 | INTRODUCTION

Atopic dermatitis (AD) is a chronic inflammatory skin disorder affecting up to 3%–5% of adults and 20% of children worldwide.[1–3] The pathophysiology of AD involves various factors including host genetics, altered skin barrier function, and immunological abnormalities.[2,4,5] A defective skin barrier and aberrant immune activation are characteristic features of AD. Immunologically, AD is considered a primarily Th2/Th22-driven disease with varying degrees of Th1/Th17 skewing.[6–8] Molecular studies of skin biopsy samples that utilized high-throughput analyses revealed their immune abnormalities. Recent advances in functional genomics technologies, including single-cell and proteomics analyses, facilitate the detailed molecular and immunological characterization of AD. Single-cell

transcriptomics has provided fundamental new insights into disease pathogenesis and the regulatory mechanisms at the molecular and cellular level.[9–12] Nevertheless, these studies lack spatial information and often suffer from reconstructing the locations of many cell types. Moreover, they cannot properly characterize cell–cell interactions to extrapolate where and how neighboring cells affect proinflammatory and transcriptional networks inside the tissue.

Although blockade of type 2 inflammation, such as an IL-4 receptor α blocking monoclonal antibody and Janus kinase inhibitors, have shown high treatment efficacy,[13–15] these agents do not work uniformly in each patient, most likely due to the heterogeneity of this disease. AD can be divided into phenotypes based on clinical factors such as severity and age of onset and endotypes such as degrees of type 2 activation and non-IgE-associated disease mechanisms. The mechanisms behind the complexity of AD are still not fully understood. Clinical trials using novel targeted treatments were instrumental to better understand AD pathogenesis.[16,17] Nevertheless, biomarkers for the stratification of patients, the prediction and monitoring of treatment responses and severity are not yet in clinical use, mandating a better understanding of the disease.

Combining two powerful transcriptomics methods: single-cell and spatial transcriptomics, we identified unique subgroups of inflammatory fibroblasts, M2 macrophages, and activated dendritic cells (DCs) that shape the cellular and molecular characteristics of skin inflammation in the leukocyte-infiltrated area of lesional skin in AD. Moreover, ligand–receptor analysis showed molecular interactions between these immuno-active cells. In addition, we showed the signature of these novel inflammatory interactions in the serum levels of circulating inflammatory proteins and correlations with AD symptom severity.

2 | METHODS

2.1 | Study design

Skin tissues examined for spatial gene expression were derived from 6 healthy control donors and 7 AD patients, which were obtained at Augsburg University Hospital with written consent. Healthy control donors—2 males and 4 females—were aged 24–63 years and had no history of skin disease. The demographics of the study population are shown in Table 1.

For single-cell analysis, suction blister material from untreated AD lesions and HC skin at the antecubital fossa skin (4 ADs and 5 HCs) were collected and $CD45^+$ cells were enriched by FACS for further analysis.[10] Enzymatically digested full-thickness skin biopsies (4 ADs and 2 HCs) were also collected and similarly enriched for $CD45^+$ (50% for each sample). The multiple proximity extension assay included 36 patients diagnosed with AD at the High-Altitude Clinic in Davos, Switzerland, and 28 HCs.[18] The included AD patients were 18–85 years of age. Bulk RNA-seq was performed from 4-mm skin biopsies of 13 chronic-phase patients with AD with a lesion in the upper arm (mean SCORAD score, 57.3; range, 32–99.5) and seven healthy control subjects.[19] Two AD and one healthy samples were excluded from analysis due to technical difficulties or low RNA yield. See the Online Repository/OR Methods for additional details.

2.2 | Visium spatial transcriptomics sequencing

Frozen human skin biopsy samples were cryosectioned and transferred onto a Visium Spatial Gene Expression Slide (10X Genomics). Tissue sections were stained with hematoxylin and eosin, and images were captured using an Axio Z1 slide scanner (Zeiss). Gene expression libraries were prepared according to the Visium Spatial Gene Expression Reagent Kits User Guide (Rev D, 10X Genomics). Visium libraries were sequenced on a NovaSeq 6000 System (Illumina) using a NovaSeq S4 Reagent Kit (200 cycles, 20,027,466, Illumina), at a sequencing depth of approximately 73–180 Mio reads per sample. The median UMI counts per spot in the raw data are 1694, and the median feature counts per spot in the raw data are 1101. Visium libraries were sequenced, and raw Binary Base Call (BCL) files were processed in Space Ranger v.1.2.0 and demultiplexed using "spaceranger mkfastq." The resulting FASTQ files were mapped to the human genome build GRCh38.p13 and annotated using the GENCODE gene annotation release 32 with "spaceranger count." Secondary analysis was performed using the Seurat R package (v4.0.3). Each sample was log-normalized using Seurat's NormalizeData function with default parameters and scaled. All samples were integrated using reciprocal principal component analysis (RPCA). For dimensionality reduction and clustering, the Louvain modularity optimization algorithm was run at a resolution of 0.1 to identify broad clusters. See the OR Methods for additional details.

TABLE 1 Demographic characteristics of the study subjects for spatial transcriptomics.

Demographics	Healthy control ($n=6$)	Atopic dermatitis ($n=7$)
Age (years; mean ± SD)	42.17 ± 17.46	39.00 ± 15.92
Female/Male	4/2	3/4
Onset month (mean ± SD; range)	—	5 ± 2.92 (1–10)
SCORAD (mean ± SD)	—	44.49 ± 13.73
EASI (mean ± SD)	—	16.90 ± 14.79
Total IgE (IU/mL; mean ± SD; range)	15 ± 7.4 (5.2–45; $n=5$)	1321 ± 2764.37 (9.2–7500; $n=6$)

Abbreviations: EASI, Eczema Area and Severity Index; SCORAD, Scoring atopic dermatitis.

2.3 | Single-cell RNA-seq reference data processing

Previously published feature-barcode matrices were obtained from Gene Expression Omnibus (Accession Nr: GSE153760) and re-analyzed and prepared as a cell-type reference with Seurat (v4.0.3). The data set was log-normalized and scaled, using the same parameters as for the spatial transcriptomics data set. Integration was performed by RPCA. We performed a two-step approach for accurate cell type identification. First-level clustering determined broad cell type categories and second-level clustering on selected subsets identified more specific cell types. The prediction scores in each spot were calculated by Seurat's label transfer method. See the OR Methods for additional details.

2.4 | Spatial differential gene expression analysis

Differential gene expression analysis was performed using the Seurat package with the function FindMarkers with "test.use" parameter set to DESeq2. Heatmap was obtained after the calculation of average expression for all of the genes in cluster 1 in each group (HC, NL, LS) using the AverageExpression function (Table S1). Volcano plots were made using EnhancedVolcano (ver. 1.12.0) R package. In addition, the distribution of the gene expression between disease status (HC, NL, and LS) in the Cluster 1 was shown in violin plots. Moreover, ligand–receptor interaction analysis was performed with the curated Ligand/Receptor Interaction Database.[20] Significantly correlated ligand–receptor pairs within Visium spots were identified with the function correlatePairs from the scran package (ver. 3.1.3) separately for the three groups (HC, NL, and LS). To further elucidate ligand–receptor interaction within specific cell types, we used a single-cell data set[10] and calculated the LRscore with a threshold of 0.5.[20] To show the colocalized ligand–receptor pairs supported by the Visium Spatial Transcriptome data, the significantly correlated pairs identified from the previous analysis with their LRscore are displayed on the heatmap (Figure 5B). The pairs with LRscore <0.5 are shown as gray in the heatmap. The average expression of selected molecules was calculated within each cell type, and the results are displayed in Figure S5B. See the OR Methods for additional details.

2.5 | RNA-sequencing in skin biopsy samples

We analyzed the database of our previous study.[19] We performed RNA-seq analysis on matched lesional and nonlesional skin tissue biopsy specimens from patients with AD ($n = 11$) and healthy subjects ($n = 6$). See the OR Methods for additional details.

2.6 | Immunohistochemistry staining

The cryosection samples from frozen tissue blocks (4 LS, 4 NL, and 4 HC) were stained with an anti-COL18A1 antibody (Abcam, ab275390, rabbit IgG, 1:200), an anti-TNC antibody (Invitrogen, MA5-16086, mouse IgG1, 1:2000), an anti-CD3 antibody (BioRad, MCA1477, rat IgG1, 1:150), an anti–CCL19 antibody (R&D Systems, MAB361–100, mouse IgG2b, 1:200), an anti–1B10 (fibroblast surface marker) antibody (Novus, NB100–1845, Mouse IgM, 1:200), an anti–CCR7 antibody (Abcam, ab253187, rabbit IgG, 1:200), an anti–CD11C antibody (Abcam, ab11029, mouse IgG1, 1:500), an anti-MMR (MRC1, CD206) antibody (NOVUS, MAB2534, rat IgG2a, 1:200), and an anti-CD45RO antibody (Biolegend, No. 304239, mouse IgG2a, κ, 1:200). See the OR Methods for additional details.

2.7 | High-throughput targeted proteomics from serum

Serum samples (29 AD patients before the treatment and 20 HC) from a previous cohort[18] were newly analyzed using another Olink Target 96 panel, named the cardiometabolic panel, by proximity extension assay (OLINK). See the OR Methods for additional details.

3 | RESULTS

3.1 | Spatial gene profiling of atopic dermatitis lesions

To explore the cell–cell interactions and the complex networks in lesion formation of AD, we performed RNA-sequencing (RNA-seq) spatial transcriptomics on nonlesional (NL) and lesional (LS) AD skins, and compared them to the skin of healthy controls (HC). We investigated the histopathological features of AD in hematoxylin and eosin images together with specific gene expression, followed by separating the spots in the Visium array into eight clusters (Figure 1A,B; Figures S1). An extracellular matrix with lower numbers of cell infiltrates and fibroblasts was identified as cluster 0, and cluster 3 consists of a denser fibroblast population. LS showed a significant expression of leukocyte infiltration at the upper dermis (cluster 1). Epidermal thickness in LS was associated with a predominant cluster in the lower epidermis (cluster 2) and upper epidermis (cluster 4). The larger number of spots in LS compared to NL and HC in the uniform manifold approximation and projection (UMAP) graphs are indicative of increased cellular infiltration, particularly leukocyte infiltrate, and high cell numbers in the lower and upper epidermis (Figure 1B). The heat map listing each cluster's top 10 most significantly differentially expressed genes shows that cluster 1 represents the leukocyte infiltration and resident immune cells with a high expression of surface proteins from the group of major histocompatibility complexes (MHC) of class II in humans such as human leukocyte antigens (*HLAs-DRA*, *HLAs-DRB1*, *HLAs-DPA1*, and *HLAs-DPB1*) and *CD74* as predominantly expressed genes (Figure 1C). Clusters 0 and 3 contain fibroblasts with the expression of collagens (*COL1A1* and *COL6A2*). Cluster 2 represents the lower epidermis with keratinocyte (*KRT5* and *KRT14*) and melanocyte (*PMEL*) markers. Cluster 4 represents the upper epidermis

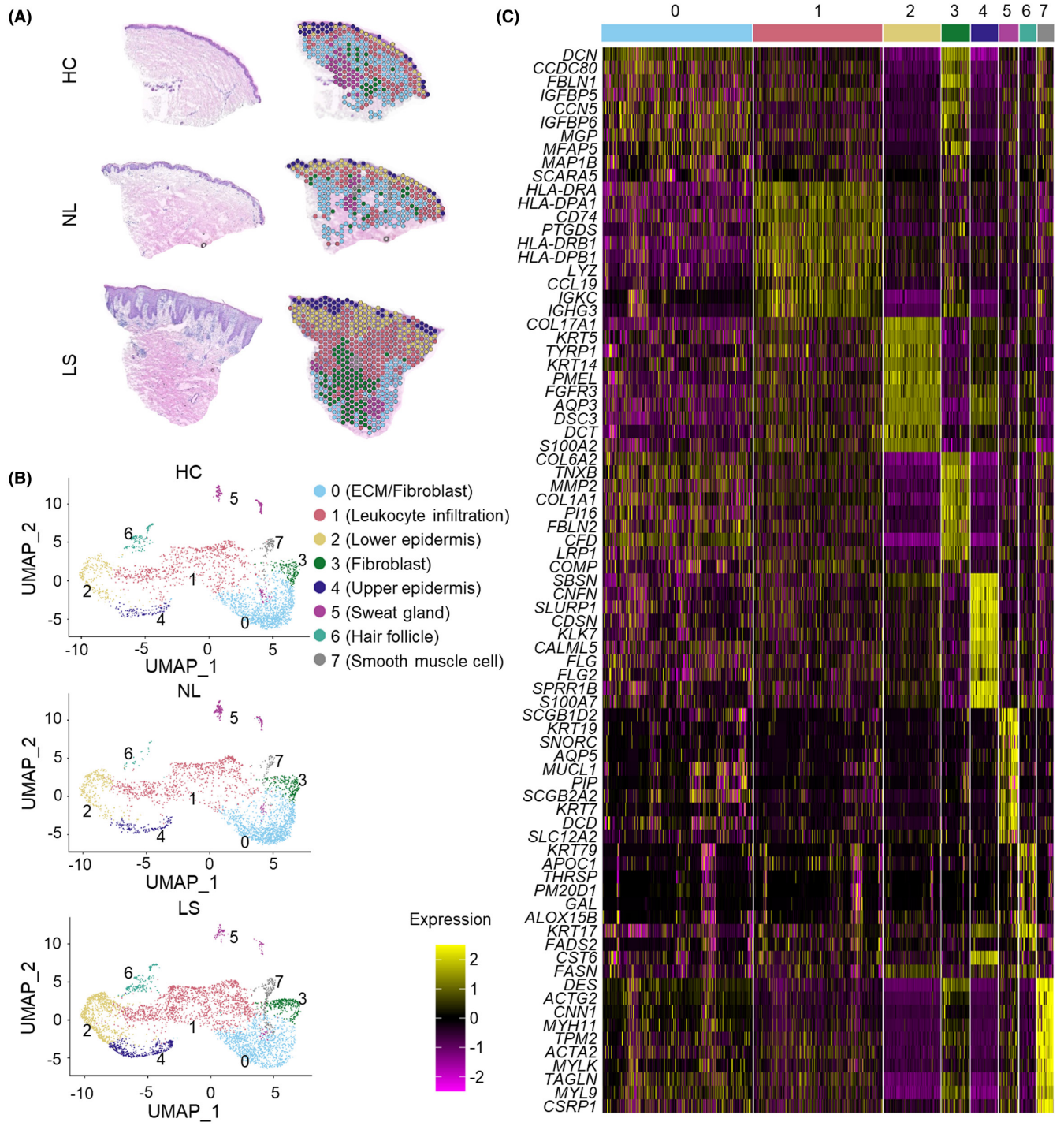

FIGURE 1 Spatial transcriptomic analyses of healthy control skin, and nonlesional and lesional skin of atopic dermatitis. (A) Hematoxylin and eosin staining and overlaid clustering of spatial transcriptomics spots of tissue sections. Clustering according to the similarity of transcriptome resulted in eight different color-coded clusters. ECM, extracellular matrix; HC, healthy control skin; LS, lesional skin; NL, nonlesional skin; (B) UMAPs of clusters separated in atopic dermatitis nonlesional skin (NL, $n=5$), lesional skin (LS, $n=7$), and skin of healthy controls (HC, $n=6$). Eight different color-coded clusters as in A. (C) Heat map displaying the top 10 differentially expressed genes for each cluster compared with the rest of the data set.

with the expression of barrier molecules, filaggrins and desmosomes (*FLG*, *FLG2*, and *CDSN*). Cluster 5 represents sweat glands with the expression of *MUCL1*, *AQP5*, and *DCD*. Cluster 6 represents hair follicles with the upregulation of *KRT79* and *KRT17*. Cluster 7 contains smooth muscle cells with the expression of *ACTA2* and *MYL9*.

3.2 | Cellular landscape of the lesions and leukocyte-infiltrated area in atopic dermatitis

To explore the phenotype and topographical distribution of the T cell and leukocyte infiltrates in AD, we integrated the spatial

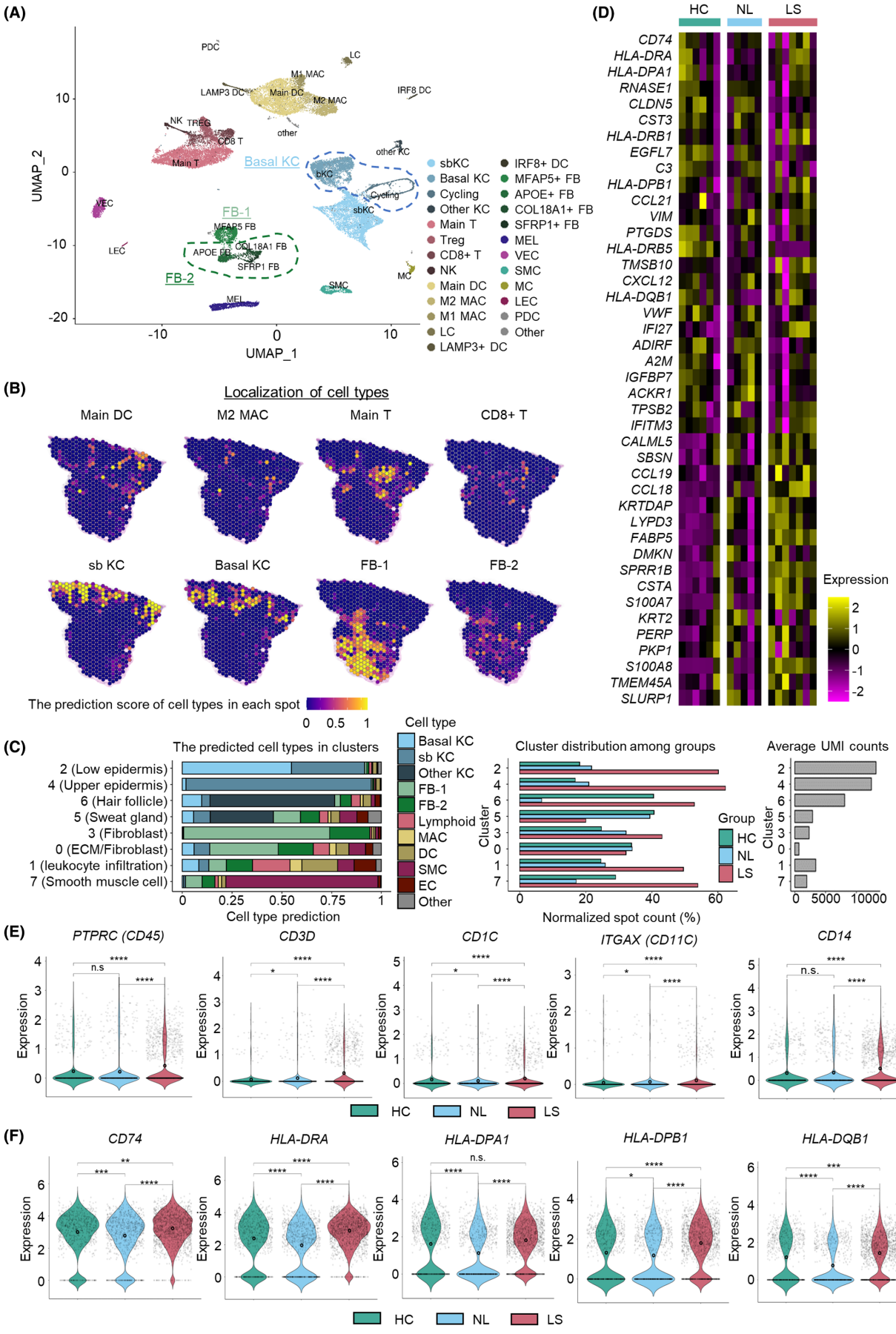

FIGURE 2 Cellular landscape of the lesions and leukocyte-infiltrated area in atopic dermatitis. (A) Single-cell RNA-seq UMAP of annotated clusters of cell types from 15 donors (four AD and five HC suction blister samples and four AD and two HC biopsy samples). DC, dendritic cells; FB, fibroblasts; LC, Langerhans cells, LEC, lymphatic endothelial cells; MAC, macrophages; MEL, melanocytes; NK, natural killer cells; PDC, plasmacytoid dendritic cells; sbKC, suprabasal keratinocytes; SMC, smooth muscle cells; Treg, regulatory T cells; VEC, vascular endothelial cells. (B) Spatial feature plots of cell type prediction scores in spatial transcriptomics of LS sections. (C) Adverse prediction scores for each cell type per cluster (left), normalized spot count of each group per cluster as percentage (middle), average UMI count per cluster (right). (D) Heat map displaying the top 20 highly expressed genes in each group within the "leukocyte infiltration" cluster compared with the rest of the data set. (E and F) Violin plots of the indicated gene expression within the leukocyte infiltration cluster. $^{*}p \le .05$, $^{**}p \le .01$, $^{***}p \le .001$, $^{****}p \le .0001$, n.s. = not significant, Wilcoxon rank-sum test.

transcriptomics data with single-cell data.[10] Each cell type was identified by the resemblance to findings in single-cell RNA-seq study of AD skin (Figure 2A; Figure S2A–D).[10] Further clustering of the single-cell data demonstrated the expression of T cells, $CD8^+$ T cells, and Treg cells. The main effector T-cell population (Main T) showed *CD3* expression and was devoid of $CD8^+$ T cell, Treg cell, and NK cell markers. $CD8^+$ T cells were similar to NK cells in the expression of *GZMB* and *NKG7* in addition to *CD3* and *CD8A*. Treg cells showed a distinct population with the expression of *FOXP3* and *CTLA4*. Myeloid cells were visible as DCs, Langerhans cells, and macrophages. $CD1C^+$ DCs were present as *LAMP3*-expressing DCs, $IRF8^+$ DCs that were also expressing *CLEC9A*, and main DCs that were *IRF8* and *LAMP3* negative. IRF8 and CLEC9A are known as the markers for conventional DC1, and LAMP3 is known as a marker of mature DCs. Type 1 macrophages (M1) are characterized by expression of proinflammatory cytokines *IL1B* and downregulation of *MRC1*. Type 2 macrophages (M2) were more dominant with the expression of *CD163* and *MRC1*.

We predicted the cell type in each spot by probabilistic label transfer of cell type annotations from single-cell RNA-seq data (Figure 2B,C). The leukocyte-infiltrated area in LS consists of DCs, M2, and T cells, located in the upper dermis layer closer to the epidermis. These cells and leukocyte infiltrate were negligible in HC and NL skin, and T cells, DCs, and macrophages were colocalizing in the leukocyte-infiltrated area in the AD lesions. Suprabasal and basal keratinocytes were located in the epidermis. We were able to divide the fibroblasts into four subgroups ($MFAP5^+$, $COL18A1^+$, $APOE^+$, and $SFRP1^+$ fibroblasts). $MFAP5^+$ fibroblasts were the main fibroblast subgroup with the expression of *MFAP5*, *FBN1*, and *WISP2*. These fibroblasts were named group 1 (FB-1). The remaining subgroups of $COL18A1^+$, $APOE^+$, and $SFRP1^+$ fibroblasts were combined as group 2 fibroblasts (FB-2).

Cluster 1 was characterized by a high probability of predicted lymphoid cells, macrophages, DCs, and endothelial cells. Clusters 2, 3, 4, 6, and 7 were predominantly defined by their respective cell type of interest. The number of spots among groups was highest in LS for clusters 1, 2, 4, and 7, showing leukocyte infiltrate and thick epidermis. The more dominant clusters 1, 2, and 4 in LS are caused by a thicker epidermal layer and denser cellular infiltration showing higher unique molecular identifier (UMI) counts. However, LS expressed relatively low numbers of cells originating from sweat glands. Cluster 3 contained mainly FB-1 fibroblasts expressing *MFAP1* as the main fibroblast cluster. The dominant fibroblast group switched in the leukocyte-infiltrated area to FB-2 (Figure 2C).

We further explored the gene expression profiles in the leukocyte-infiltrated area in three groups (HC, NL, and LS) in comparison (Figure S3A). The heat map in Figure 2D shows the top 20 significantly upregulated genes in cluster 1 for each group (Figure S3B). Genes that are characteristic of endothelial cells (*VWF* and *CLDN5*) were expressed in all groups, suggesting that this cluster includes capillaries (Figure 2D). We identified that the gene expression of *CCL18*, *CCL19*, and *CCL21* was highly upregulated especially in the leukocyte-infiltrated area in lesions. The leukocyte marker genes, such as *PTPRC* (CD45), *CD3D*, *CD1C*, *ITGAX* (CD11C), and *CD14*, are shown prominently in the cluster 1 and these leukocytes are prominently increased in lesional AD skin and CD3D, CD1C, and CD11C are already increased in the nonlesional AD skin. (Figure 2E). In addition, MHC class II-related molecules (*CD74*, *HLA-DRA*, *HLA-DRB5*, *HLA-DPA1*, and *HLA-DQB1*) were downregulated in NL compared to HC and LS, suggesting that the antigen-presentation capacity of MHC class II-expressing cells is downregulated in NL (Figure 2F).

3.3 | Identification of activated fibroblasts and dendritic cells in the leukocyte-infiltrated area in lesional skin

The RNA-seq analyses of full-thickness skin biopsies from previous independent AD cohorts[19] detected increased gene expression of *CCL19*, *CCR7*, *CCL17*, *CCL22*, and *TNC* in LS (Figure 3A). *CCL19* was one of the top upregulated genes in the leukocyte-infiltrated area in LS compared to HC (Figure S3A). To explore how distinct cell types may contribute to immune activity through the expression of the ligand–receptor couple *CCL19* and *CCR7* in AD, we investigated the subgroups of cell types in our single-cell data set. The *CCL19*- and *CCR7*-expressing cell types were monitored in LS of AD (Figure 3B). Many cell types, including basal keratinocytes and smooth muscle cells, express CCL19 in the skin. $COL18A1^+$ fibroblasts and $LAMP3^+$ DCs are the top two sources of CCL19. $LAMP3^+$ DCs are the predominant cell types among CCR7-positive cells, which may suggest an interaction between these two cell types.

After the detection of $CCL19^+$ $COL18A1^+$ fibroblasts and $CCR7^+$ $LAMP3^+$ DCs, we further determined the location of each cell type in the leukocyte-infiltrated area in LS. We identified that gene expression of extracellular matrix (*COL6A5*, *COL4A1*, *COL4A2*, and *TNC*) and proinflammatory cytokines/chemokines (*IL32* and *CCL19*) were highly upregulated in $COL18A1^+$ fibroblasts from

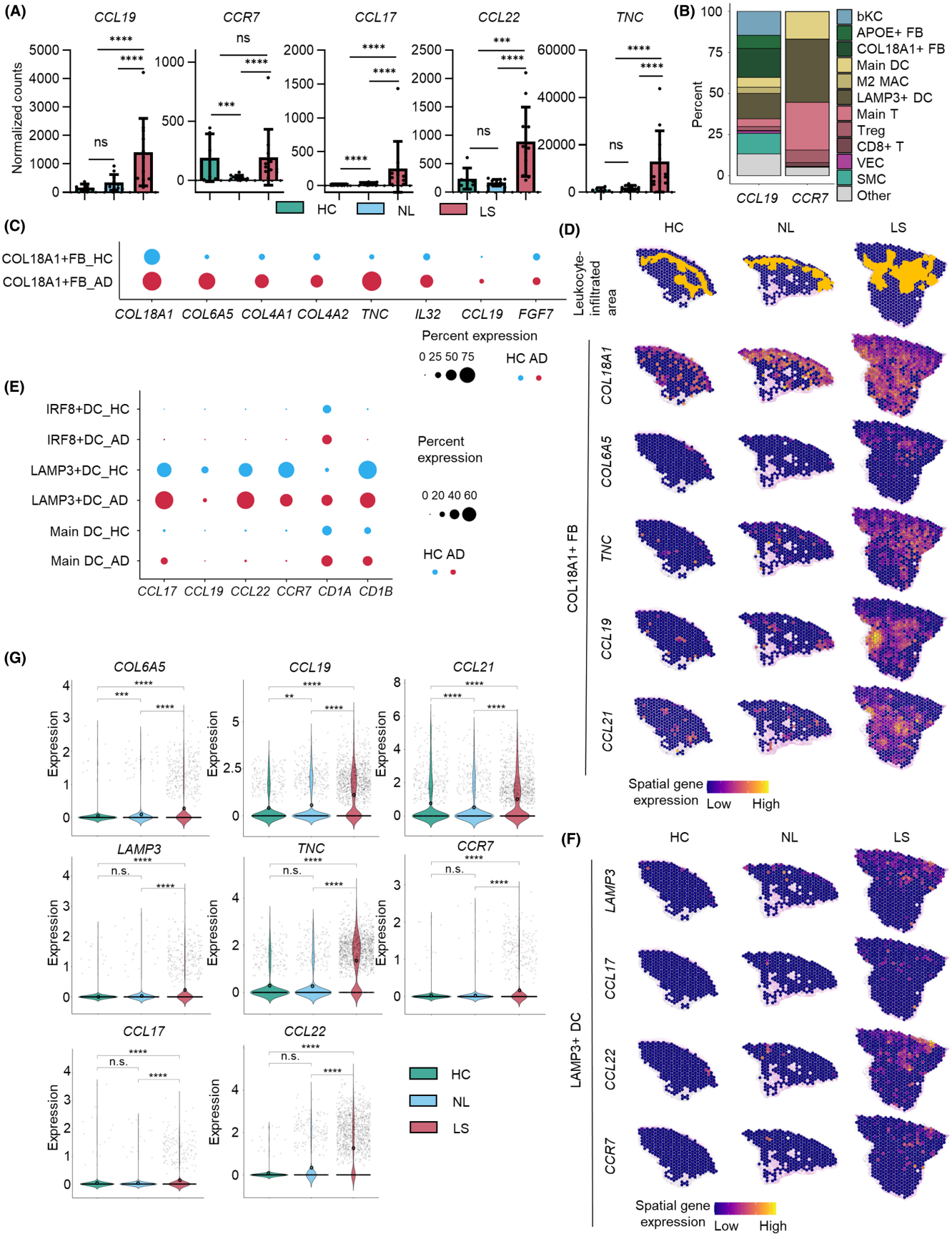

FIGURE 3 Characterization of dendritic cells and fibroblasts in atopic dermatitis by spatial/single-cell transcriptomics. (A) Bar plots of bulk RNA-seq depicting the gene expression of indicated AD-related genes in the skin comparing healthy control (HC, $n=6$), nonlesional AD (NL, $n=11$), and lesional AD (LS, $n=11$). Each dot indicates the expression level in an individual. Normalized counts are shown. Graph shows mean with SD. $^{***}p \le .001$, $^{****}p \le .0001$, n.s. = not significant, edgeR. (B) Stacked bar graph depicting the distribution of *CCL19* (left) and *CCR7* (right) expressing cells among all identified cell types in the AD subset of the single-cell RNA-seq data. bKC, basal keratinocytes; DC, dendritic cells; FB, fibroblasts; MAC, macrophages; SMC: smooth muscle cells; Treg, regulatory T cells; VEC, vascular endothelial cells. (C) Gene expression dot plots of single-cell RNA-seq showing the expression frequencies of selected genes in COL18A1$^+$ fibroblasts (blue: healthy control, red: atopic dermatitis). Distinct gene signatures of other fibroblasts subpopulations are depicted in Figure S4A. (D) Spatial feature plots of expression of cluster-specific marker genes of COL18A1$^+$ fibroblasts. The leukocyte-infiltrated area is highlighted as yellow area on blank sections. (E) Gene expression dot plots of single-cell RNA-seq data of dendritic cell subpopulations. (F) Spatial feature plots of cluster-specific marker genes of LAMP3$^+$ DCs. (G) Violin plots of the indicated gene expression within the leukocyte infiltration cluster. $^{**}p \le .01$, $^{***}p \le .001$, $^{****}p \le .0001$, n.s. = not significant. Wilcoxon rank-sum test.

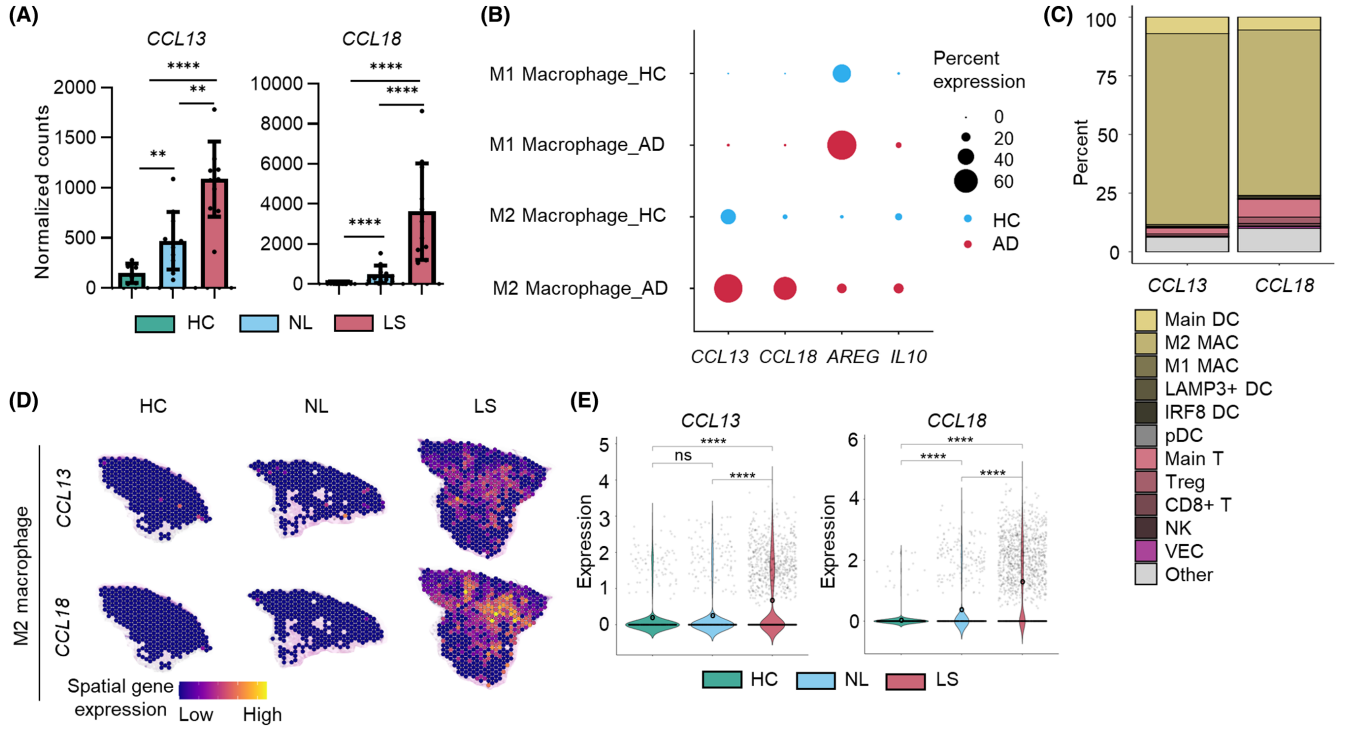

FIGURE 4 Identification of CCL13- and CCL18-expressing M2 macrophages in atopic dermatitis. (A) Bar plots of bulk RNA-seq depicting the gene expression of *CCL13* and *CCL18* in the skin comparing healthy control (HC, $n=6$), nonlesional AD (NL, $n=11$), and lesional AD (LS, $n=11$). Each dot represents an individual. Normalized counts are shown. Graph shows mean with SD. $^{**}p \le .01$, $^{****}p \le .0001$, edgeR. (B) Gene expression dot plots of single-cell RNA-seq showing the expression frequencies of selected genes in M1 and M2 macrophages (blue: healthy control, red: atopic dermatitis). (C) Stacked bar graph depicting the distribution of *CCL13* (left) and *CCL18* (right) expressing cells among all identified cell types in the AD subset of the single-cell RNA-seq data. DC, dendritic cells; MAC, macrophages; NK, Natural killer cell; pDC, plasmacytoid dendritic cells; Treg, regulatory T cells; VEC, vascular endothelial cells. (D) Spatial feature plots of cluster-specific marker genes of M2 macrophage. (E) Violin plots of the indicated markers in gene expression within the leukocyte infiltration cluster. Each dot shows the expression level in individual spots. $^{****}p \le .0001$, n.s. = not significant. Wilcoxon rank-sum test.

AD (Figure 3C; Figure S4A). These extracellular matrix and proinflammatory cytokines/chemokines expressing fibroblasts are activated fibroblast in AD skin. On the contrary, APOE$^+$ fibroblasts and MFAP5$^+$ fibroblasts had a higher expression of *FGF7*, which was more pronounced in AD lesions compared to HC. Importantly, COL18A1$^+$ fibroblasts were found across the whole dermis, but activated COL18A1$^+$ fibroblasts were particularly localized in the leukocyte-infiltrated area in LS and colocalized with LAMP3$^+$ DCs (Figure 3D–F). *COL4A1* and *COL4A2* were also upregulated in the leukocyte-infiltrated area in the skin lesions; however, other collagens such as COL6A1 did not follow this trend (Figure S4B,C). Although TNC was more broadly expressed, it was also accumulated in the same area. In addition to this LAMP3$^+$ DCs and COL18A1$^+$ fibroblasts interaction area, *CCL19* showed additional hot spots which warrant further investigation.

We were able to discern spatial information of DCs in AD skin. We found that *CCL17*, *CCL22*, and *CCR7* were highly expressed in LAMP3$^+$ DCs, but were not significantly different in the skin from HC and AD individuals (Figure 3E). LAMP3$^+$ DCs appeared not only in the leukocyte-infiltrated area in LS, but also partially on

the surface of epidermal layers (Figure 3F). It should be noted that Langerhans cells do not express *LAMP3* (Figure S2D). These results suggest that most of the professional antigen-presentation is taking place in the dermis and that some activated LAMP3^{+} DCs exist very close to the surface of the epidermis. Figure 3G shows all of these fibroblast- and DC-related genes were upregulated in LS.

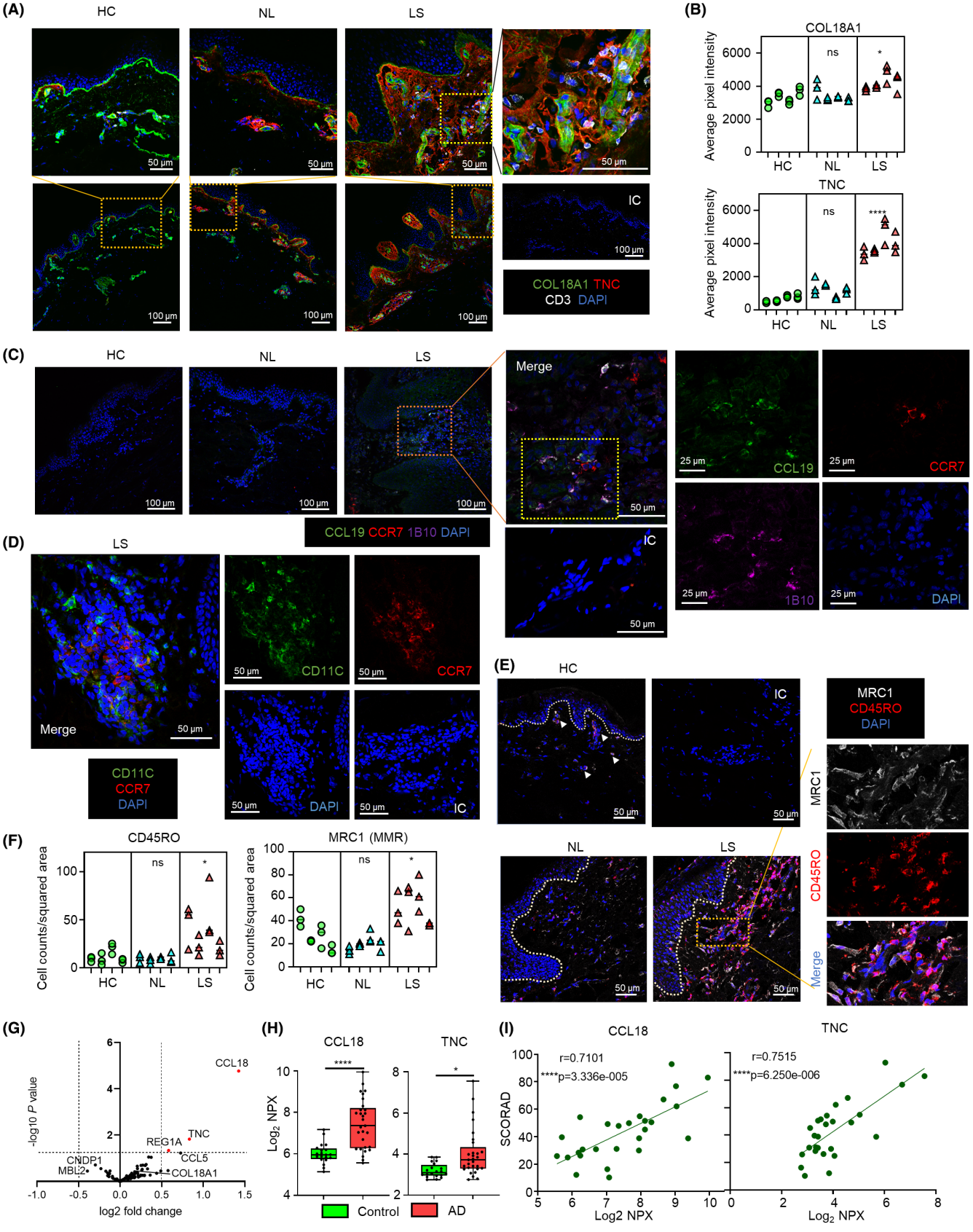

FIGURE 5 Demonstration of the cellular activation and interaction between COL18A1$^+$ fibroblasts, M2 macrophages, and T cells in AD. (A) Example images of the expression of COL18A1 (green), TNC (red), CD3 (white), and DAPI (blue) in three visual fields per individual donors (healthy control; HC, $n=4$, nonlesional skin of AD: NL, $n=4$, and lesional skin of AD: LS, $n=4$). The bottom images depict the low magnifications with isotype control (IC) on the bottom right and the images on the top row depict the zoomed in areas in orange dotted box. Top right picture shows the highest magnification view of yellow dotted box in the lesional skin on the top row. The scale bars (white line) are 50 μm (top) and 100 μm (bottom). (B) Quantification of average pixel intensity of COL18A1 fibroblasts and TNC in the skin. Each plot depicts the intensity of randomly selected square images. *$p \leq .05$, ****$p \leq .0001$, n.s. = not significant, one-way ANOVA. (C) Example images of the expression of CCL19 (green), CCR7 (red), IB10 (magenta), and DAPI (blue) in three visual fields per individual donors. The middle images depict the zoomed-in areas in the orange dotted box with isotype control (IC) on the bottom. The images on the right show the results of indicated staining of the yellow dotted box. The scale bars (white line) are 100 μm (left), 50 μm (middle), and 25 μm (right). (D) Example images of the expression of CD11C (green), CCR7 (red), and DAPI (blue) in the lesional skin. The merged image is shown with the results of indicated staining with isotype control (IC). The scale bars (white line) are 50 μm. (E) Example images of the expression of CD45RO (red), MRC1 (white), and DAPI (blue). The large images on the right side depict the individual markers and the merged image of the zoomed-in area of the orange box. The scale bar (white line) is 50 μm. Dotted lines denote the position of the basement membrane. Arrowheads indicate the MRC1$^+$ cells in HC skin. (F) The numbers of CD45RO$^+$ cells and MRC1$^+$ cells in the skin. Each plot depicts the cell counts of CD45RO and MRC1 in randomly selected square images. *$p \leq .05$, n.s. = not significant, one-way ANOVA. (G) Volcano plot of the Olink proteomics data comparing the healthy control data ($n=20$) to that from patients with AD ($n=29$). p value ≤.05 and log2 fold change ≥|0.5| were taken as a significance threshold. The significantly differentially regulated genes are shown as red dots. Moderated t-test. (H) Box plots of selected molecules are shown. Normalized protein expression (NPX) is shown on a log2 scale. Whiskers indicate minimum to max value. *$p \leq .05$, ****$p \leq .0001$, Moderated t-test. (I) Correlation of Protein NPX of indicated molecules and SCORAD. ****$p \leq .0001$. The Pearson correlation coefficient r and p values (two-tailed) are shown.

3.4 | Spatial characterization of atopic dermatitis lesion-infiltrating macrophages

CCL18 was one of the top upregulated genes in the leukocyte-infiltrated area in LS (Figure S3A). Accordingly, we investigated the source of *CCL18* in the skin of AD patients. Recently, it was reported that CD14$^+$ macrophages expressed inflammatory cytokines including *CCL13* and *CCL18*.[9,10] Whole skin biopsies showed that expression of *CCL13* and *CCL18* was significantly upregulated both in NL and LS from AD patients compared to HC (Figure 4A). M1 macrophages expressed the EGFR ligands amphiregulin (*AREG*), but did not express *CCL13* and *CCL18* (Figure 4B). The spatial gene expression of *AREG* was also upregulated in LS (Figure S4D,E). We identified M2 macrophages by their high expression of *CD163* and *MRC1*, also known as *CD206* or *MMR*. The single-cell analysis showed that M2 macrophages showed high expression of *CCL13* and *CCL18* only in AD lesions (Figure 4B,C). Colocalized spatial gene expression of *CCL13* and *CCL18* showed activated M2 macrophages in the leukocyte-infiltrated area in LS (Figure 4D). Expression of M2-related genes was upregulated in LS (Figure 4E).

3.5 | The levels of tissue and circulating serum proteins related to fibroblasts, DCs and macrophages correlate with the severity of AD

The localization of TNC expressing COL18A1$^+$ fibroblasts and M2 macrophages within skin was further investigated using immunofluorescence and immunohistochemistry. We stained the skin biopsy samples from the same donors that we used for our spatial transcriptomics analysis by anti- COL18A1, TNC, and CD3 antibodies (Figure 5A). COL18A1$^+$ fibroblasts were identified in the dermis and at the basement membrane in all groups. COL18A1 and TNC co-expressing spindle-shaped cells are detected in the leukocyte-infiltrated area (the high magnification picture of yellow dotted square in Figure 5A). Importantly, TNC was localized particularly around COL18A1 expressing cells in the skin of AD patients, and it is significantly increased in LS (Figure 5B). We further investigated the cellular crosstalk in the leukocyte-infiltrated area. CCR7-expressing cells are shown in the leukocyte-infiltrated area in lesional skin and are located in the close proximity with CCL19-expressing 1B10$^+$ (fibroblast surface marker) fibroblasts (Figure 5C). In addition, these CCR7-expressing cells do not express CCL19. Figure 5D shows the co-expression of CCR7 and CD11C. Some of the CCR7-expressing cells are CD11C positive DCs. The rest of CCR7-expressing cells are supposed to be CD11C-negative DC or T cells according to the single-cell transcriptome data (Figure 3B). We found CD3$^+$ T cells infiltrating around COL18A1$^+$ fibroblasts. Moreover, we found MRC1, which is known as macrophage mannose receptor (MMR), and CD45RO positive cell infiltration into lesional AD skin. CD45RO$^+$ subsets of T cells and MRC1$^+$ subsets of macrophages were in close proximity (Figure 5E). Furthermore, frequencies of both subsets were higher in samples from AD lesions (Figure 5F).

To investigate whether this cellular signature was paralleled by a distinct serum biomarker expression pattern, we used proteomic multiplex data from serum samples of AD patients. We analyzed the expression of 92 biomarkers and we identified the increase of three biomarkers (CCL18, TNC, REG1A) but not COL18A1 in the serum of AD patients compared to the serum from control (Figure 5G,H). We also re-analyzed our current multi proteomics study data[18] and serum levels of CCL19 and AREG were significantly upregulated in AD (Figure S4F). Importantly, serum levels of CCL18, TNC, and AREG in AD patients showed a significant correlation with the scoring atopic dermatitis (SCORAD)[21] (Figure 5I; Figure S4G). These results suggest a systemic impact of the proinflammatory skin microenvironment in AD.

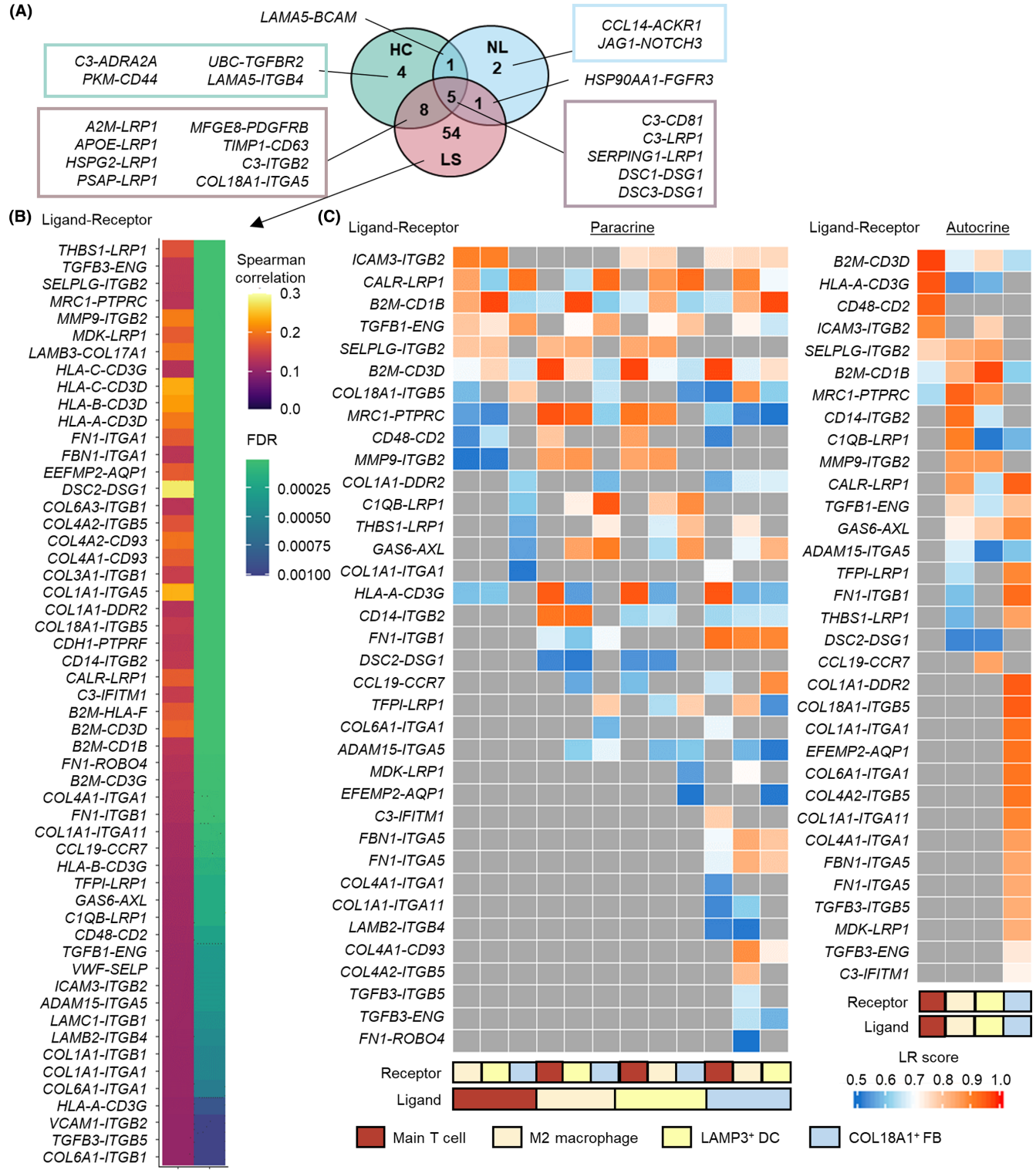

FIGURE 6 Cellular crosstalk landscape between dendritic cells, macrophages, fibroblasts, and T cells in atopic dermatitis. (A) The Venn diagram depicting the shared or unique significantly correlated ligand–receptor pairs between leukocyte-infiltrated clusters in healthy control (HC), nonlesional (NL), and lesional (LS) AD skin ($p \leq .05$, |log2 fold change|>0). (B) Heatmap of spatial gene expression analysis depicting ligand–receptor pairs enriched only in the leukocyte-infiltrated cluster in AD lesion with the Spearman correlation rate and the false discovery rate (FDR). The threshold of significance is FDR <.001. (C) Heatmap of single-cell gene expression analysis depicting ligand–receptor pairs across subclusters of cell types. Paracrine (left) and autocrine (right) interactions are shown with LR score. LR score of <.5 is indicated in gray. Correction for multiple hypothesis testing was performed with the Benjamini–Hochberg procedure, and the threshold for significance was set to .05.

3.6 | Ligand–receptor interactions in the leukocyte-infiltrated areas in AD lesional skin

As we observed an extensive colocalization of DCs, macrophages, fibroblasts, and T cells, we investigated the interacting ligand–receptor pairs between these cells. A Venn diagram depicts the number of ligand–receptor pairs that were significantly correlated in each group in our data of spatial transcriptomics (Figure 6A). The leukocyte-infiltrated area in LS shows 68 ligand–receptor pairs, of which 54 of them are specific for AD lesions. Of these, 13 of them overlap with HC and 6 of them overlap with NL. The Gene ontology (GO) term analysis of these pairs demonstrates that the expression of leukocyte chemotaxis, cytokine-mediated signaling pathway, and extracellular matrix organization-related ligand–receptor pairs were significantly correlated within the Visium spots of LS, but not in HC or NL (Figure 6B; Figure S5A). These ligand–receptor pairs included *CCL19-CCR7*, *COL4A1-CD93*, *MRC1-PTPRC*, and the interactions of β2 microglobulin and HLA-A/B/C with *CD3* and *CD1B*. Figure 6C and Figure S5B show the expression of ligands and receptors in each cell type and their correlations at the single-cell level. Results are split in two different types of cell–cell interaction, namely in a paracrine and autocrine modes. In these heatmaps, we can observe that COL18A1$^+$ fibroblasts and LAMP3$^+$ DCs or LAMP3$^+$ DCs themselves are the main sources of *CCL19-CCR7* pairs. A correlation between the *COL4A1-CD93* pair indicates the possible interaction between COL18A1$^+$ fibroblasts and M2 macrophages. *CD14-ITGB2* and *MRC1-PTPRC* pairs represent a significant interaction between M2 macrophages and T cells in the leukocyte-infiltrated area in LS. We demonstrated the *CCL19-CCR7* interaction in the leukocyte-infiltrated area in LS by using spatial images and ligand–receptor analysis. Additionally, we showed a positive correlation between *COL18A1*, *COL4A1*, *COL4A2* and their receptors in this area. The *CD3D/G-B2M*, *CD3D/G-HLA-A/B/C*, and *CD2-CD48* pairs indicate that interactions between T cells and antigen-presenting cells may be taking place. Moreover, other ligand–receptor pairs such as *C3-IFITM1* point to an interaction between COL18A1$^+$ fibroblasts and T cells. *VCAM1-ITGB2* and *VWF-SELP* pairs may indicate that endothelial cells in the leukocyte-infiltrated area attract leukocytes into lesions. These results suggest that positively correlated ligand- or receptor-expressing cell pairs exist nearby in leukocyte infiltration in LS and have functions in chemotaxis, antigen-presentation, and T-cell activation. These data define novel molecular interactions between fibroblasts, macrophages, DCs, and T cells in the leukocyte-infiltrated area in LS, which may play a central role in the lesion formation and inflammation of AD.

4 | DISCUSSION

In the present study, the integration of spatial transcriptomics and single-cell transcriptomics in skin biopsies allowed us to dissect cellular localization, as well as to identify novel cell subsets, expression of novel molecules, and interaction between neighboring cells. Several recent studies have demonstrated the complex inflammatory characteristics of the AD skin.[22–26] In addition, recently reported single-cell RNA-seq analyses provided a wealth of information on skin-infiltrating cell subsets and demonstrate the clear difference between AD and psoriasis,[27,28] but there was a lack of information on spatial and neighboring cells, particularly in the leukocyte infiltrating area.[9,10,29,30] Spatial transcriptomics enables us to molecularly characterize transcriptomes of the specific localizations.[31–33] In this study, we provide cell-type resolution of gene expression properties and identify the detailed characteristics of leukocyte infiltrations and resident tissue cells and the interactions between them. Another important contribution of the current study is that all of the presented data demonstrate the direct in vivo analysis without using cell cultures, as the data are based on analyses of affected tissues and serum of patients. We demonstrate that fibroblasts, macrophages, and DCs show AD lesion-specific transformations, and may interact not only with each other but also with T cells in skin lesions. These cell types and their specifically interacting ligand or receptor molecules are not expressed in unaffected skin of AD patients, suggesting that these interactions have developed in association with skin lesion formation. In addition, we highlight the potential targets of ligand–receptor pairs for drug development that characterize the cross-talk between these cells. The reflection of the expression of these molecules in peripheral blood suggests their potential use as biomarkers of inflammation and disease severity.

A compelling finding of the present study is the observed change in the fibroblasts characteristics that also play a role as lymphoid tissue organizer-like function during lesion formation. COL18A1$^+$ fibroblasts are located in the whole dermis of healthy skin, and apparently, they changed their phenotype by expressing *CCL19*, *TNC*, *COL6A5*, *COL4A1*, and *COL4A2* especially in the leukocyte-infiltrated area in lesions. Prior to the present study, the interactions between fibroblasts and DCs in vivo in the skin have not been studied in detail. It was recently reported by single-cell transcriptomics that COL6A5$^+$ and COL18A1$^+$ fibroblasts upregulate *CCL19* and may attract CCR7 positive DCs and T-cell populations into AD skin lesions.[9] Reynaud. et al. also detected CCL19-expressing fibroblasts and CCR7-expressing DC population in the skin of AD patients in their single-cell study.[28] Here, we demonstrate that activation of COL18A1$^+$ fibroblasts are specific for the leukocyte-infiltrated area in lesions and that they most likely interact with neighboring DCs and macrophages. *CCR7* is a chemokine receptor for the *CCL19* ligand that is expressed mainly on T cells and semi-mature/mature DCs.[34] A *Dermatophagoides farinae* body extract-induced mouse model of AD showed upregulation of *Ccr7* in skin DCs.[35] It has been reported that CCL19$^+$, CCL21$^+$ stromal cells, called lymphoid tissue organizer cells recruit CCR7$^+$ lymphocytes and myeloid cells into secondary lymphoid organs.[36,37] Similarly, in inflammatory bowel disease, *CCL19*$^+$ and *CCL21*$^+$ stromal cells have recently been identified in single-cell analysis.[38] These kinds of lymphoid tissue organizer-like cells induce tertiary lymphoid structures (TLSs) formation in chronic inflammatory tissues.[36] He et al. demonstrated that the CCL19-expressing COL18A1$^+$ COL6A5$^+$ fibroblast, LAMP3$^+$ CCR7$^+$ DC,

and CCL13$^+$ CCL18$^+$ macrophages by single-cell RNA sequencing.[9] In the present study, we contributed some additional points, such as the change of their phenotype between healthy and AD skin, cells in their close proximity and interaction between their ligands and receptors as well as the serum levels of their activated markers. Spatial transcriptomics provided more evidence on the interaction of the cells in addition to single-cell transcriptomics. We identified upregulation of *CCL19* and *CCL21* in the leukocyte-infiltrated area in AD skin lesions. In addition, we present images of spatial gene expression of activated *CCL19*-expressing COL18A1$^+$ fibroblasts and *CCR7*-expressing LAMP3$^+$ DC subsets in the leukocyte-infiltrated area in LS. Moreover, we showed that CCR7-expressing cells infiltration into the leukocyte-infiltrated area in lesional skin and are located in the close proximity with CCL19-expressing fibroblasts. Our data may suggest that these CCL19-expressing fibroblasts and CCR7-expressing cells represent TLSs. Importantly, our ligand–receptor interaction analysis identified the expression of *COL18A1*, *COL4A1*, *COL4A2*, *CCL19* and their receptors, and revealed that there was a significant correlation in the cell–cell interactions within the leukocyte-infiltrated area in LS.

Although the functions of *COL6A5*, *COL4A1*, and *COL4A2* are currently elusive, it has been reported that polymorphisms located in *COL6A5*, *COL8A1*, and *COL10A1* may be linked to disease susceptibility in AD in a Mediterranean cohort.[39] Depletion of *Ikkb* in Prx1$^+$ fibroblasts induce AD-like skin lesions and show the upregulation of *Col6A5* in conditional knockout mouse.[40] *COL4A1* and *COL4A2* are used as common fibrosis markers.[41] Development of fibrosis and avoidance of severe fibrosis are important elements both taking place in the AD skin.[42] TNC is an element of the extracellular matrix of various tissues, including the skin, and is involved in modulating the extracellular matrix integrity and cell physiology.[43] The present study demonstrates that TNC expression is increased around COL18A1$^+$ fibroblasts especially in the leukocyte-infiltrated area in the lesional skin. This is in agreement with previous studies showing that TNC is upregulated in the lesional skin of AD.[44] However, TNC's potential as a biomarker is currently not well explored. We showed upregulation of tissue and serum levels of TNC may reflect the activation of COL18A1$^+$ fibroblasts in lesions of AD. In addition, our findings suggest that these molecules may serve as potential biomarkers for disease activity. Different fibroblast subtypes show different characteristics. MFAP5$^+$ or APOE$^+$ fibroblasts express more *FGF7* compared to COL18A1$^+$ fibroblasts. *FGF7*, also known as keratinocyte growth factor, modulates keratinocyte viability, proliferation, and differentiation.[45] Recently, the various types of heterogeneity in fibroblasts have been characterized at a single-cell resolution in multiple organs and previous studies suggest that they can gain pathological features that drive disease progression and persistence.[36,46] Supporting this concept, an increased subpopulation of fibroblasts in fibrotic skin diseases interact with type 2 responses have been reported.[47,48]

Macrophages represent an important component of leukocyte infiltrations in lesions due to their molecular interactions with other cells. Stimuli such as IL-4, IL-10, IL-13, and TGF-β favor macrophage polarization to M2 subpopulation,[49] which plays a central role in response to parasites, tissue remodeling, angiogenesis, and allergic diseases. It has been reported that IL-4, IL-13, or IL-10-activated M2 macrophages induce CCL18 expression and histamine further facilitates the expression of CCL18 in activated M2 macrophages.[50] Type 2 inflammation, mediated by IL-4 and IL-13, plays an essential role in AD. Because spatial transcriptome is prone to incomplete detection of genes expressed at low levels, we can estimate their existence by detecting downstream molecules, such as chemokines. CCL13 and CCL18 are known as type 2 chemokines. Here, we identified CCL13- and CCL18-expressing M2 subpopulations in the leukocyte-infiltrated area in LS that show similar distribution with AD-specific fibroblasts, DCs, and T cells. Zhang et al. also reported increased expression of CCL13 and CCL18 in the macrophage along with AD severity[27] Rapamycin, which is a macrolide compound, downregulates the release of CCL13 and CCL18 from IL-4-treated macrophages and inhibits *Dermatophagoides farinae* body antigen-induced dermatitis in NC/Nga mice.[51] M2 macrophages may represent a potential target for the mTOR inhibitors; rapamycin, cyclosporine, and tacrolimus. Of note, serum levels of CCL18 were increased in AD patients and showed a significant correlation with the severity of AD. Dupilumab (anti-IL4 receptor α antibody) significantly decreased the levels of CCL18 in serum from AD patients.[14] It has been reported that the serum levels of CCL13 were upregulated in AD and correlated with barrier dysfunction.[18] These studies may lead to the identification of novel biomarkers to monitor AD to predict exacerbations and follow-up of response to therapy.

In this study, we present data that suggest antigen-presentation is taking place inside the dermis as a TLS-like cellular infiltrate. These molecular interactions may play a central role in the lesion formation of AD. We demonstrate that skin-infiltrating T cells show a cross-talk with surrounding cells through CD3D, CD3G, and their receptor pairs, such as HLA molecules between the T cells and fibroblasts, macrophages, or DCs. In addition, *CD48* and its receptor *CD2* expressed on T cells show the interaction between T cells and antigen-presenting cells. *CD14*, *MRC1*, and their corresponding receptor pairs indicate that M2 macrophages significantly interact with T cells, and LAMP3$^+$ DCs in the leukocyte-infiltrated area in LS. PTPRC, also known as CD45, is a transmembrane glycoprotein expressed on almost all hematopoietic cells. CD45RO is known as one of the isoforms which is expressed on CD4$^+$ memory T lymphocyte subset and activated T lymphocytes. Our immunohistochemistry and spatial transcriptomics results demonstrate that there is a potential cellular crosstalk between CD45RO$^+$ T lymphocytes and M2 macrophage in lesions. The establishment of TLS in human skin at sites of inflammation, which may play a key role as pathogenic hubs of acquired immune responses, has been reported in the skin.[52,53] However, the formation of TLS in AD skin has not been fully understood. The findings in this study suggest the formation of TLS and local antigen-presentation is taking place in the skin.

In addition, our findings demonstrate specific ligand–receptor interactions that facilitate leukocyte infiltration in the dermis. *CCL19-CCR7* interaction in the leukocyte-infiltrated area involves CCR7$^+$ T-cell interaction with COL18A1$^+$ fibroblasts and LAMP3$^+$ DCs, and

there is a higher interaction between these DCs and fibroblasts. This interaction may also play an important role in the formation of a TLS in the dermis.[54] Additionally, we show that COL18A1$^+$ fibroblasts start to express molecules that are involved in cellular cross-talk, such as *COL4A1*, *COL4A2*, and *CCL19* in the lesional skin. The analyses of healthy skin demonstrate that COL18A1$^+$ fibroblasts do not express these molecules in non-atopic individuals, suggesting that their differentiation in the AD skin is taking place to stimulate the CCR7 and CCL19 interaction, and maybe one of the initiating factors to attract DC and T cells into the leukocyte-infiltrated area in the dermis. ITGB2, which is known as lymphocyte function associated antigen 1, shows the interaction with ICAM3 and VCAM1. These pairs contribute to lymphocyte-endothelial cell interactions. Identification of *VWF-SELP* pair suggests that the leukocyte recruitment into lesions are activated by P-selectins expressed on the endothelial cells.

Despite the multitude of novel findings highlighted in this study, it does have some limitations. First, the Visium assay has a resolution of 55 μm diameter in each spot and therefore detects 2–10 cells in the spots adding to the heterogeneity of the results. The differences in cell density, which were shown as differences in average UMI counts, led to spillover gene detection in the dermis from the epidermis. This is the reason why the heatmap in Figure 2D includes some keratin markers. However, the extensive statistical analyses of every individual spot and combined with other Visium spots helped us reduce this noise and identify molecular interactions between the cells. If there was only one cell per spot, we would not have the advantage to identify cellular cross-talks in such detail. Second, we identified cell types through the alignment with previously published single-cell data,[9,10] which allowed us to predict constituent-cell types in each cluster. Some cell types known to be involved in AD pathogenesis, for example, mast cells, have not been investigated in this study. Third, it is not easy to separate autocrine from paracrine interaction in ligand–receptor analysis, because those results rely on the pooled predictions of cellular cross-talk. Fourth, our study involved instantaneous and single time point analyses of the lesions, which is one of the main shortcomings of almost all previous studies due to the limitation of taking sequential biopsies from patients. Future research efforts should focus on longitudinal analyses of the skin biopsies and further development of the techniques used towards a higher resolution.

Taken together, the combination of spatial transcriptomics, single-cell transcriptomics, and proteomics analyses enabled a detailed characterization of skin lesions and the TLS in the dermis, namely the leukocyte infiltrate and cellular cross-talk between the involved cells. We demonstrated unique molecular interactions between AD lesion-specific *CCL19*-, *TNC*-, *COL6A5*-, *COL18A1*-expressing fibroblasts, *CCR7*- and *LAMP3*-expressing DCs, *CCL13*- and *CCL18*-expressing M2 macrophages, and T cells in the leukocyte-infiltrated area of skin lesions. Our findings provide a comprehensive in-depth knowledge of the nature of AD skin lesions.

AUTHOR CONTRIBUTIONS

Yasutaka Mitamura and Cezmi A. Akdis conceived and conceptualized the project. Matthias Reiger, Arturo O. Rinaldi, and Claudia Traidl-Hoffmann performed the sample collection. Yasutaka Mitamura and Juno Kim performed spatial transcriptomics experiments and targeted multiple proteomics experiment. Patrick M. Brunner performed the single-cell transcriptomics experiment. Beate Rücker performed the immunohistochemistry experiments. Yasutaka Mitamura, Juno Kim, Yi Xiao, Damir Zhakparov, Ge Tan, Katja Baerenfaller, and Damian Roqueiro interpreted and visualized data. Mübeccel Akdis, Marie-Charlotte Brüggen, Kari C. Nadeau, Patrick M. Brunner, Damian Roqueiro, Claudia Traidl-Hoffmann and Cezmi A. Akdis supervised the project. Yasutaka Mitamura and Cezmi A. Akdis wrote the manuscript. Katja Baerenfaller, Patrick M. Brunner, Damian Roqueiro, and Claudia Traidl-Hoffmann edited the manuscript.

ACKNOWLEDGMENTS

This work was supported by the FreeNovation grant from Novartis Research Foundation (FreeNovation 2020), Basel and by the Christine Kühne Center for Allergy Research and Education (CK-CARE). Yasutaka Mitamura and Marie-Charlotte Brüggen are members the research consortium SKINTEGRITY.CH. We thank Anja Heider for their help in the laboratory and Anna Głobińska for her help in preparing the figures. Yasutaka Mitamura was supported financially by EAACI with a EAACI Research Fellowship 2019, the Fellowship of Astellas Foundation for Research on Metabolic Disorders, Japanese Dermatological Association with JDA Grant-In-Aid for Study Abroad 2020, and Mochida Memorial Foundation for Medical and Pharmaceutical Research. Marie-Charlotte Brüggen received financial support from LEO foundation. Claudia Traidl-Hoffmann received financial support from the Initiative and Networking Fund (Immunology & Inflammation) of the Helmholtz Association. Yi Xiao, Damir Zhakparov and Katja Baerenfaller were supported financially by the Center for Data Analysis, Visualization and Simulation (DAViS) that is funded by the Swiss canton of Grisons. Open access funding provided by Universitat Zurich.

FUNDING INFORMATION

FreeNovation grant from Novartis (YM).

CONFLICT OF INTEREST STATEMENT

YM reports grants from Novartis and financial support from EAACI, Astellas Foundation for Research on Metabolic Disorders, Japanese Dermatological Association, and Mochida Memorial Foundation. MR reports personal fees from Bencard, Germany, La Roche Posay, Germany, Galderma, Germany, Sebapharma, Germany, grants from CLR, Germany, and Beiersdorf, Germany, outside the submitted work. KCN reports grants from National Institute of Allergy and Infectious Diseases (NIAID), National Heart, Lung, and Blood Institute (NHLBI), National Institute of Environmental Health Sciences (NIEHS), and Food Allergy Research & Education (FARE); stock options from IgGenix, Seed Health, ClostraBio, and ImmuneID; is Director of the World Allergy Organization Center of Excellence for Stanford, Advisor at Cour Pharma, Consultant for Excellergy, Red tree ventures, Eli Lilly, and Phylaxis, Co-founder of Before Brands, Alladapt, Latitude, and IgGenix; and National Scientific Committee

member at Immune Tolerance Network (ITN), and National Institutes of Health (NIH) clinical research centers, outside the submitted work; patents include, "Mixed allergen composition and methods for using the same," "Granulocyte-based methods for detecting and monitoring immune system disorders," and "Methods and Assays for Detecting and Quantifying Pure Subpopulations of White Blood Cells in Immune System Disorders." PMB has received personal fees from Almirall, Sanofi, Janssen, Amgen, LEO Pharma, AbbVie, Pfizer, Boehringer Ingelheim, GSK, Regeneron, Eli Lilly, Celgene, Arena Pharma, Novartis, UCB Pharma, BMS, and Biotest, and received research support from Pfizer. CTH reports personal fees from Novartis, Germany, La Roche Posay, Germany Sanofi, Germany, Lilly pharma, Germany, Lancome, Germany, L'O real, Germany, grants and personal fees from Töpfer GmbH, Danone Nutricia, Sebapharma, and Beiersdorf AG, Germany, outside the submitted work. C. A. Akdis has received research grants from the Swiss National Science Foundation, European Union (EU CURE, EU Syn-Air-G), Novartis Research Institutes, (Basel, Switzerland), Stanford University (Redwood City, Calif), and SciBase (Stockholm, Sweden); is the Co-Chair for EAACI Guidelines on Environmental Science in Allergic diseases and Asthma; is on the Advisory Boards of Sanofi/Regeneron (Bern, Switzerland, New York, USA), Stanford University Sean Parker Asthma Allergy Center (CA, USA), Novartis (Basel, Switzerland), Glaxo Smith Kline (Zurich, Switzerland), Bristol-Myers Squibb (New York, USA), Seed Health (Boston, USA), and SciBase (Stockholm, Sweden); and is the Editor-in-Chief of Allergy.

DATA AVAILABILITY STATEMENT

All data associated with this study are in the paper or the Supplementary Materials. The accession number for the raw and processed sequencing data reported in this paper is Gene Expression Omnibus (GEO): GSE153760 (single-cell analysis) and GSE197023 (spatial transcriptomics analysis). Analysis scripts for spatial transcriptomics and single-cell transcriptomics analyses are available at https://gitlab.com/juno.kim/visium-atopic-dermatitis. Analysis scripts for proteomics analysis are available at https://github.com/ge11232002/OlinkR. Analysis scripts for RNA-seq analyses are available at https://github.com/uzh/ezRun.

ORCID

Yasutaka Mitamura https://orcid.org/0000-0001-6389-9285
Matthias Reiger https://orcid.org/0000-0002-6173-2104
Juno Kim https://orcid.org/0000-0002-1388-4787
Ge Tan https://orcid.org/0000-0003-0026-8739
Katja Baerenfaller https://orcid.org/0000-0002-1904-9440
Mübeccel Akdis https://orcid.org/0000-0003-0554-9943
Marie-Charlotte Brüggen https://orcid.org/0000-0002-8607-6254
Kari C. Nadeau https://orcid.org/0000-0002-2146-2955
Damian Roqueiro https://orcid.org/0000-0002-9195-5915
Claudia Traidl-Hoffmann https://orcid.org/0000-0001-5085-5179
Cezmi A. Akdis https://orcid.org/0000-0001-8020-019X

REFERENCES

1. Asher MI, Montefort S, Björkstén B, et al. Worldwide time trends in the prevalence of symptoms of asthma, allergic rhinoconjunctivitis, and eczema in childhood: ISAAC phases one and three repeat multicountry cross-sectional surveys. *Lancet*. 2006;368(9537):733-743.
2. Langan SM, Irvine AD, Weidinger S. Atopic dermatitis. *Lancet*. 2020;396(10247):345-360.
3. Barbarot S, Auziere S, Gadkari A, et al. Epidemiology of atopic dermatitis in adults: results from an international survey. *Allergy*. 2018;73(6):1284-1293.
4. Hülpüsch C, Weins AB, Traidl-Hoffmann C, Reiger M. A new era of atopic eczema research: advances and highlights. *Allergy*. 2021;76(11):3408-3421.
5. Lunjani N, Tan G, Dreher A, et al. Environment-dependent alterations of immune mediators in urban and rural south African children with atopic dermatitis. *Allergy*. 2021;77:569-581.
6. Renert-Yuval Y, Thyssen JP, Bissonnette R, et al. Biomarkers in atopic dermatitis-a review on behalf of the international eczema council. *J Allergy Clin Immunol*. 2021;147(4):1174-1190.e1171.
7. Pavel AB, Zhou L, Diaz A, et al. The proteomic skin profile of moderate-to-severe atopic dermatitis patients shows an inflammatory signature. *J Am Acad Dermatol*. 2020;82(3):690-699.
8. Nomura T, Kabashima K. Advances in atopic dermatitis in 2019–2020: endotypes from skin barrier, ethnicity, properties of antigen, cytokine profiles, microbiome, and engagement of immune cells. *J Allergy Clin Immunol*. 2021;148(6):1451-1462.
9. He H, Suryawanshi H, Morozov P, et al. Single-cell transcriptome analysis of human skin identifies novel fibroblast subpopulation and enrichment of immune subsets in atopic dermatitis. *J Allergy Clin Immunol*. 2020;145(6):1615-1628.
10. Rojahn TB, Vorstandlechner V, Krausgruber T, et al. Single-cell transcriptomics combined with interstitial fluid proteomics defines cell type-specific immune regulation in atopic dermatitis. *J Allergy Clin Immunol*. 2020;146(5):1056-1069.
11. Tibbitt CA, Stark JM, Martens L, et al. Single-cell RNA sequencing of the T helper cell response to house dust mites defines a distinct gene expression signature in airway Th2 cells. *Immunity*. 2019;51(1):169-184.e165.
12. Hughes TK, Wadsworth MH II, Gierahn TM, et al. Second-Strand synthesis-based massively parallel scRNA-seq reveals cellular states and molecular features of human inflammatory skin pathologies. *Immunity*. 2020;53(4):878-894.e877.
13. Simpson EL, Bieber T, Guttman-Yassky E, et al. Two phase 3 trials of dupilumab versus placebo in atopic dermatitis. *N Engl J Med*. 2016;375(24):2335-2348.
14. Guttman-Yassky E, Bissonnette R, Ungar B, et al. Dupilumab progressively improves systemic and cutaneous abnormalities in patients with atopic dermatitis. *J Allergy Clin Immunol*. 2019;143(1):155-172.
15. Guttman-Yassky E, Teixeira HD, Simpson EL, et al. Once-daily upadacitinib versus placebo in adolescents and adults with moderate-to-severe atopic dermatitis (measure up 1 and measure up 2): results from two replicate double-blind, randomised controlled phase 3 trials. *Lancet*. 2021;397(10290):2151-2168.
16. Ratchataswan T, Banzon TM, Thyssen JP, Weidinger S, Guttman-Yassky E, Phipatanakul W. Biologics for treatment of atopic dermatitis: current status and future Prospect. *J Allergy Clin Immunol Pract*. 2021;9(3):1053-1065.
17. Bieber T. Atopic dermatitis: an expanding therapeutic pipeline for a complex disease. *Nat Rev Drug Discov*. 2021;1-20:21-40.
18. Rinaldi AO, Korsfeldt A, Ward S, et al. Electrical impedance spectroscopy for the characterization of skin barrier in atopic dermatitis. *Allergy*. 2021;76(10):3066-3079.
19. Altunbulakli C, Reiger M, Neumann AU, et al. Relations between epidermal barrier dysregulation and staphylococcus

species-dominated microbiome dysbiosis in patients with atopic dermatitis. *J Allergy Clin Immunol*. 2018;142(5):1643-1647 e1612.
20. Cabello-Aguilar S, Alame M, Kon-Sun-Tack F, Fau C, Lacroix M, Colinge J. SingleCellSignalR: inference of intercellular networks from single-cell transcriptomics. *Nucleic Acids Res*. 2020;48(10):e55.
21. Oranje AP, Glazenburg EJ, Wolkerstorfer A, de Waard-van der Spek FB. Practical issues on interpretation of scoring atopic dermatitis: the SCORAD index, objective SCORAD and the three-item severity score. *Br J Dermatol*. 2007;157(4):645-648.
22. Esaki H, Brunner PM, Renert-Yuval Y, et al. Early-onset pediatric atopic dermatitis is T(H)2 but also T(H)17 polarized in skin. *J Allergy Clin Immunol*. 2016;138(6):1639-1651.
23. Suárez-Fariñas M, Ungar B, Correa da Rosa J, et al. RNA sequencing atopic dermatitis transcriptome profiling provides insights into novel disease mechanisms with potential therapeutic implications. *J Allergy Clin Immunol*. 2015;135(5):1218-1227.
24. Brunner PM, He H, Pavel AB, et al. The blood proteomic signature of early-onset pediatric atopic dermatitis shows systemic inflammation and is distinct from adult long-standing disease. *J Am Acad Dermatol*. 2019;81(2):510-519.
25. Brunner PM, Israel A, Leonard A, et al. Distinct transcriptomic profiles of early-onset atopic dermatitis in blood and skin of pediatric patients. *Ann Allergy Asthma Immunol*. 2019;122(3):318-330.e313.
26. Brunner PM, Suárez-Fariñas M, He H, et al. The atopic dermatitis blood signature is characterized by increases in inflammatory and cardiovascular risk proteins. *Sci Rep*. 2017;7(1):8707.
27. Zhang B, Roesner LM, Traidl S, et al. Single-cell profiles reveal distinctive immune response in atopic dermatitis in contrast to psoriasis. *Allergy*. 2022;78:439-453.
28. Reynolds G, Vegh P, Fletcher J, et al. Developmental cell programs are co-opted in inflammatory skin disease. *Science*. 2021;371(6527):eaba6500.
29. Alkon N, Bauer WM, Krausgruber T, et al. Single-cell analysis reveals innate lymphoid cell lineage infidelity in atopic dermatitis. *J Allergy Clin Immunol*. 2021;149:624-639.
30. Rindler K, Krausgruber T, Thaler FM, et al. Spontaneously resolved atopic dermatitis shows melanocyte and immune cell activation distinct from healthy control skin. *Front Immunol*. 2021;12:630892.
31. Tavares-Ferreira D, Shiers S, Ray PR, et al. Spatial transcriptomics of dorsal root ganglia identifies molecular signatures of human nociceptors. *Sci Transl Med*. 2022;14(632):eabj8186.
32. Ji AL, Rubin AJ, Thrane K, et al. Multimodal analysis of composition and spatial architecture in human squamous cell carcinoma. *Cell*. 2020;182(2):497-514.e422.
33. Srivatsan SR, Regier MC, Barkan E, et al. Embryo-scale, single-cell spatial transcriptomics. *Science*. 2021;373(6550):111-117.
34. Hauser MA, Legler DF. Common and biased signaling pathways of the chemokine receptor CCR7 elicited by its ligands CCL19 and CCL21 in leukocytes. *J Leukoc Biol*. 2016;99(6):869-882.
35. Yoshida Y, Hayakawa K, Fujishiro M, et al. Social defeat stress exacerbates atopic dermatitis through downregulation of DNA methyltransferase 1 and upregulation of C-C motif chemokine receptor 7 in skin dendritic cells. *Biochem Biophys Res Commun*. 2020;529(4):1073-1079.
36. Davidson S, Coles M, Thomas T, et al. Fibroblasts as immune regulators in infection, inflammation and cancer. *Nat Rev Immunol*. 2021;21(11):704-717.
37. Chai Q, Onder L, Scandella E, et al. Maturation of lymph node fibroblastic reticular cells from myofibroblastic precursors is critical for antiviral immunity. *Immunity*. 2013;38(5):1013-1024.
38. Kinchen J, Chen HH, Parikh K, et al. Structural remodeling of the human colonic mesenchyme in inflammatory bowel disease. *Cell*. 2018;175(2):372-386.e317.
39. Strafella C, Caputo V, Minozzi G, et al. Atopic eczema: genetic analysis of COL6A5, COL8A1, and COL10A1 in Mediterranean populations. *Biomed Res Int*. 2019;2019:3457898.
40. Ko KI, Merlet JJ, DerGarabedian BP, et al. NF-κB perturbation reveals unique immunomodulatory functions in Prx1(+) fibroblasts that promote development of atopic dermatitis. *Sci Transl Med*. 2022;14(630):eabj0324.
41. Xie T, Wang Y, Deng N, et al. Single-cell deconvolution of fibroblast heterogeneity in mouse pulmonary fibrosis. *Cell Rep*. 2018;22(13):3625-3640.
42. Gieseck RL 3rd, Wilson MS, Wynn TA. Type 2 immunity in tissue repair and fibrosis. *Nat Rev Immunol*. 2018;18(1):62-76.
43. Choi YE, Song MJ, Hara M, et al. Effects of tenascin C on the integrity of extracellular matrix and skin aging. *Int J Mol Sci*. 2020;21(22):8693.
44. Ogawa K, Ito M, Takeuchi K, et al. Tenascin-C is upregulated in the skin lesions of patients with atopic dermatitis. *J Dermatol Sci*. 2005;40(1):35-41.
45. Russo B, Brembilla NC, Chizzolini C. Interplay between keratinocytes and fibroblasts: a systematic review providing a new angle for understanding skin fibrotic disorders. *Front Immunol*. 2020;11:648.
46. Hutton C, Heider F, Blanco-Gomez A, et al. Single-cell analysis defines a pancreatic fibroblast lineage that supports anti-tumor immunity. *Cancer Cell*. 2021;39(9):1227-1244.e1220.
47. Deng CC, Hu YF, Zhu DH, et al. Single-cell RNA-seq reveals fibroblast heterogeneity and increased mesenchymal fibroblasts in human fibrotic skin diseases. *Nat Commun*. 2021;12(1):3709.
48. Boothby IC, Kinet MJ, Boda DP, et al. Early-life inflammation primes a T helper 2 cell-fibroblast niche in skin. *Nature*. 2021;599:667-672.
49. Atri C, Guerfali FZ, Laouini D. Role of human macrophage polarization in inflammation during infectious diseases. *Int J Mol Sci*. 2018;19(6):1801.
50. Mommert S, Schaper JT, Schaper-Gerhardt K, Gutzmer R, Werfel T. Histamine increases Th2 cytokine-induced CCL18 expression in human M2 macrophages. *Int J Mol Sci*. 2021;22(21):11648.
51. Mercalli A, Calavita I, Dugnani E, et al. Rapamycin unbalances the polarization of human macrophages to M1. *Immunology*. 2013;140(2):179-190.
52. Debes GF, McGettigan SE. Skin-associated B cells in health and inflammation. *J Immunol*. 2019;202(6):1659-1666.
53. Natsuaki Y, Egawa G, Nakamizo S, et al. Perivascular leukocyte clusters are essential for efficient activation of effector T cells in the skin. *Nat Immunol*. 2014;15(11):1064-1069.
54. Brandum EP, Jørgensen AS, Rosenkilde MM, Hjortø GM. Dendritic cells and CCR7 expression: an important factor for autoimmune diseases, chronic inflammation, and cancer. *Int J Mol Sci*. 2021;22(15):8340.

SUPPORTING INFORMATION

Additional supporting information can be found online in the Supporting Information section at the end of this article.

How to cite this article: Mitamura Y, Reiger M, Kim J, et al. Spatial transcriptomics combined with single-cell RNA-sequencing unravels the complex inflammatory cell network in atopic dermatitis. *Allergy*. 2023;00:1-17. doi:10.1111/all.15781